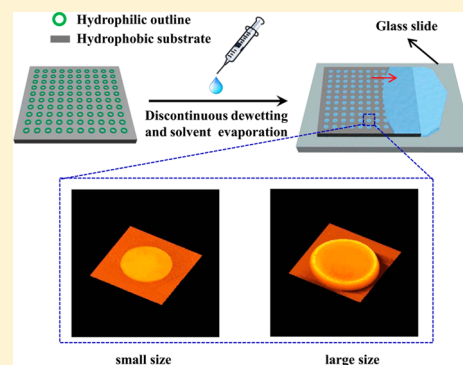


## Preparation of Patterned Ultrathin Polymer Films

Huige Yang,<sup>†,‡</sup> Meng Su,<sup>†,‡</sup> Kaiyong Li,<sup>†,‡</sup> Lei Jiang,<sup>†</sup> Yanlin Song,<sup>†</sup> Masao Doi,<sup>§</sup> and Jianjun Wang<sup>\*,†</sup><sup>†</sup>Beijing National Laboratory for Molecular Sciences (BNLMS), Key Laboratory of Green Printing, Institute of Chemistry, Chinese Academy of Sciences, Beijing 100190, PR China<sup>‡</sup>University of Chinese Academy of Sciences, Beijing 100049, PR China<sup>§</sup>Center of Soft Matter Physics and its Application, Beihang University, Beijing 100191, PR China

## S Supporting Information

**ABSTRACT:** Though patterned ultrathin polymer films (<100 nm) are of great importance in the fields of sensors and nanoelectronic devices, the fabrication of patterned ultrathin polymer films remains a great challenge. Herein, patterned ultrathin polymer films are fabricated facilely on hydrophobic substrates with different hydrophilic outline patterns by the pinning of three-phase contact lines of polymer solution on the hydrophilic outlines. This method is universal for most of the water-soluble polymers, and poly(vinyl alcohol) (PVA) has been selected as a model polymer due to its biocompatibility and good film-forming property. The results indicate that the morphologies of ultrathin polymer films can be precisely adjusted by the size of the hydrophilic outline pattern. Specifically, patterned hydrophilic outlines with sizes of 100, 60, and 40  $\mu\text{m}$  lead to the formation of concave-shaped ultrathin PVA films, whereas uniform ultrathin PVA films are formed on 20 and 10  $\mu\text{m}$  patterned substrates. The controllabilities of morphologies can be interpreted through the influences of the slip length and coffee ring effect. Theoretical analysis shows that when the size of the hydrophilic outline patterns is smaller than a critical value, the coffee ring effect disappears and uniform patterned ultrathin polymer films can be formed for all polymer concentrations. These results provide an effective methodology for the fabrication of patterned ultrathin polymer films and enhance the understanding of the coffee ring effect.



## INTRODUCTION

The patterned ultrathin polymer film is an essential component of advanced devices such as novel chemical/biological sensors and nanoelectronic devices<sup>1–3</sup> and plays a significant role in the performance of these devices. The sensitivity of a sensor can be dramatically increased with the decreasing thickness of the patterned ultrathin/microstructured polymer film, and its response time can be simultaneously decreased, resulting in the extension of application fields of advanced devices.<sup>1,4</sup> The mobility of a polymer chain on a hydrophobic substrate is higher than that on a hydrophilic substrate, leading to a higher level of polymer ordering and the associated enhanced carrier mobility of the patterned ultrathin polymer film on a hydrophobic substrate.<sup>5–7</sup> The heightened carrier mobility can markedly improve the display performance of nanoelectronic devices.<sup>2</sup> On the basis of the above-mentioned factors, the use of the hydrophobic substrate for the preparation of a patterned ultrathin polymer film is of significant importance in improving the performance of advanced devices. However, the fabrication of a continuous, microstructured, and ultrathin polymer film of arbitrary shape at a designed location through the solution process remains a challenging task due to the necessary compromise of the film thickness, the microstructure, and the formation of continuous films.<sup>1</sup> Moreover, the liquid manipulation on the highly hydrophobic surfaces is a

great challenge because the fluid nature of solution is contradictory to the formation of a liquid layer on these surfaces.<sup>8,9</sup>

The patterned polymer thin films with the desired morphology in the designated location can be prepared through various techniques<sup>10,11</sup> which pave the way for the preparation of patterned ultrathin polymer films, such as the controlled dewetting of polymer solution on the heterogeneous substrates,<sup>12,13</sup> the repeated “stick–slip” motion of three-phase contact lines through controlling the evaporation of polymer solutions confined in curve-on-flat geometry,<sup>14</sup> and the physical confinement.<sup>15</sup> The discontinuous dewetting,<sup>16</sup> which relies upon the large contrast of wettability between the hydrophilic and the hydrophobic region on the patterned substrate, is another straightforward and cost-effective technique for generating a patterned polymer thin film. McCarthy et al.<sup>17</sup> performed two series of experiments demonstrating that water droplets can be pinned on the hydrophobic surfaces by using the combinations of hydrophilic outlines of different shapes and sizes.

Received: July 6, 2014

Revised: July 24, 2014

Published: July 27, 2014

In the present work, we exploit the pinning of the three-phase contact line of polymer solution by the hydrophilic outlines patterned on the hydrophobic substrate to fabricate patterned ultrathin polymer films on the hydrophobic substrate. Hydrophobic substrates patterned with thin hydrophilic outlines of a circle, square, and equilateral triangle are prepared. During the discontinuous dewetting of poly(vinyl alcohol) (PVA) solution, the three-phase contact line is first pinned on the hydrophilic outlines, forming droplets only in the hydrophobic domains confined by hydrophilic outlines. Subsequently, the evaporation of solvent results in the formation of patterned continuous ultrathin polymer films on the hydrophobic substrate. Moreover, the patterned ultrathin polymer films do not rupture after solvent evaporation, even after storage at room temperature for 1 year.

## EXPERIMENTAL SECTION

**Preparation of Polymer Solution.** Poly(vinyl alcohol) (86–89% hydrolyzed,  $M_w = 57\,000$ – $66\,000$ , Alfa Aesar) was dissolved in a mixture of ethanol and ultrapure water (2:1 v/v) to prepare polymer solution with varying concentrations (25, 35, and 45 mg/mL). The ultrapure water was provided by a Milli-Q reference system.

**Fabrication of Chemically Patterned Substrates.** Silicon wafers were patterned by a UV light exposure technique that transferred the computer-predesigned pattern onto the photoresist-coated silicon wafer. After irradiation and development, the silicon wafers were treated by  $O_2$  plasma and then placed in a desiccator together with a Petri dish containing 1H,1H,2H,2H-perfluorodecyltrichlorosilane (FAS-17) (Alfa Aesar). The desiccator was evacuated, and the sample was kept in the desiccator for 12 h at room temperature. Then the sample was taken out and baked in a vacuum oven at  $120\text{ }^\circ\text{C}$  for 2 h. Finally, the photoresist was stripped with acetone. Hydrophobic substrates patterned with the hydrophilic outlines of a circle, square, and equilateral triangle with sizes of 100, 60, 40, 20, and  $10\text{ }\mu\text{m}$  were obtained. These hydrophilic outlines were formed into the periodic arrays over surface areas of  $1\text{ cm}^2$ .

**Preparation of Patterned Ultrathin Polymer Films.** First, the patterned substrate was placed on a glass slide. PVA solution was then carefully deposited onto the chemically patterned substrate and spread over the whole patterned substrate. After the PVA solution was disturbed with tweezers, the solution rolled along the patterned substrate and the discontinuous dewetting of PVA solution occurred, forming droplets only in the hydrophobic domains confined by hydrophilic outlines. Subsequently, the evaporation of solvent results in the formation of the patterned ultrathin polymer films as shown in Figure 1a.

**Characterization.** The static contact angle (CA) was measured at room temperature with a CA System (DSA100, Kruss Co., Germany). An optical microscope (Olympus BX51) was used to capture images of the patterned substrates without stripping the photoresist and the corresponding ultrathin PVA films. The topographical images of the patterned ultrathin PVA films were acquired by using atomic force microscopy (AFM) (SPA400, Japan NSK) in tapping mode. The viscosity of the polymer solution was measured with a digital viscometer (SNB-1, Shanghai Nirun Intelligent Technology Co. Ltd., China).

## RESULTS AND DISCUSSION

As shown in Figure 1a, we have designed patterned hydrophilic outlines on the hydrophobic substrates to control the three-phase contact lines of polymer films. During the discontinuous dewetting of polymer solution, the three-phase contact line of polymer solution is first pinned on the hydrophilic outline and polymer solution spreads over the hydrophobic domains, forming droplets only in the hydrophobic domains confined by hydrophilic outlines. Subsequently, the evaporation of solvent

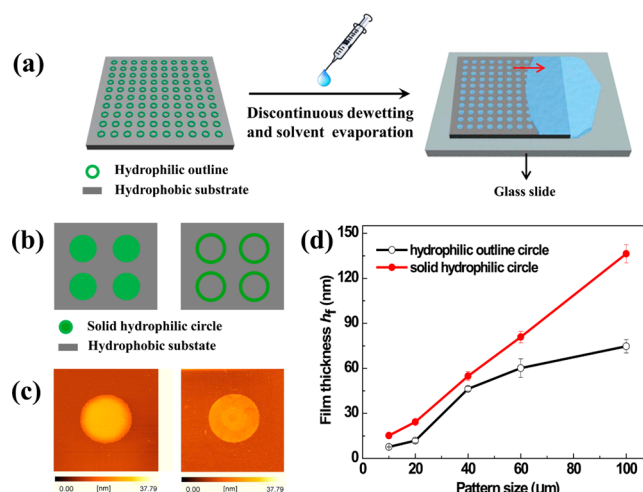


**Figure 1.** (a) Schematic representation showing the fabrication process of the patterned ultrathin polymer films on the hydrophobic substrate with the hydrophilic outlines. The red arrow indicates the direction of discontinuous dewetting, and the glass slide works as a mechanical support. (b, c) Schemes of the hydrophobic substrates patterned with the solid hydrophilic circles and hydrophilic circle outlines (b) and the corresponding AFM images ( $20 \times 20\text{ }\mu\text{m}^2$ ) of the PVA films obtained from PVA solution (35 mg/mL) (c). (d) Film thicknesses of the patterned PVA films, obtained from PVA solution (35 mg/mL), formed on the hydrophobic substrates patterned with solid hydrophilic circles and hydrophilic circle outlines with a range of sizes.

results in the formation of the patterned continuous ultrathin polymer films due to its viscosity.<sup>18</sup> As compared to the hydrophobic substrates patterned with hydrophilic outlines, the hydrophobic substrates patterned with solid hydrophilic circles are also prepared (Figure 1b), and the corresponding AFM images ( $20 \times 20\text{ }\mu\text{m}^2$ ) of the patterned PVA films are shown in Figure 1c. From the AFM images, we then measured film thicknesses of the patterned PVA films formed on the hydrophobic substrates patterned with solid hydrophilic circles and hydrophilic outlines with a range of sizes (Figure 1d). Figure 1d shows that as the sizes of the patterns are smaller than  $60\text{ }\mu\text{m}$ , the ultrathin PVA films can also be formed on the hydrophobic substrates patterned with solid hydrophilic circles. However, the results of Figure 1d indicate that the patterned PVA films induced by hydrophilic outlines are much thinner than those caused by solid hydrophilic circles for all sizes of patterns that we used. The physical basis for the differences in the film thicknesses of the patterned PVA films formed on the two types of substrates could be interpreted as follows. The slip length is defined as the distance between the solid–liquid interface and the point where the shear velocity gradient extrapolates to zero,<sup>19</sup> which indicates that the shear velocity of solution at the solid–liquid interface is positively correlated with the slip length. Since the slip length on the hydrophobic domain is larger than that on the hydrophilic domain, the velocity of shear flow in the direction of discontinuous dewetting on the outline-patterned substrate is higher than that on the solid-patterned substrate.<sup>19–21</sup> Therefore, the trapped solution on the outline-patterned substrate is lower than that on the solid-patterned substrate after discontinuous dewetting, resulting in much thinner patterned PVA films induced by hydrophilic outlines as compared to those caused by solid hydrophilic circles. This result represents strong evidence

that the strategy used to fabricate the patterned ultrathin polymer film on the hydrophobic substrate is feasible.

In order to investigate the influence of the shapes and sizes of the hydrophilic outlines on the morphology and thickness of a patterned ultrathin polymer film, we designed hydrophilic outlines of a circle, square, and equilateral triangle on hydrophobic substrates. The sizes of three types of hydrophilic outlines,  $R$ , which refer to the diameter of the circle and the side length of the square and equilateral triangle, are 100, 60, 40, 20, and 10  $\mu\text{m}$ . After being irradiated with UV light and developed, the silicon wafers were treated with  $\text{O}_2$  plasma and then modified with FAS-17, yielding the hydrophobic substrates except for the patterned area covered by the photoresist. Figure S1 in the Supporting Information shows optical images of three types of patterned substrates before stripping off the photoresist. Finally, the hydrophilic outlines were obtained by stripping off the photoresist. The contact angles of the hydrophilic outline and hydrophobic substrate were  $48 \pm 1.7$  and  $105 \pm 2.6^\circ$ , respectively. Because the substrate used in this work is a hydrophobic surface patterned with hydrophilic outlines, polymer solution cannot spread throughout the whole substrate by merely using water (high surface tension) as the solvent. On the other hand, when ethanol (low surface tension) is merely used as the solvent, the polymer solution cannot move along the patterned substrate and discontinuous dewetting cannot occur. Therefore, we chose a mixture of ethanol and water in a volume ratio of 2:1, which is selected among various volume ratios of 3:1, 2:1, 3:2, 1:1, 2:3, 1:2, 1:3, and 1:4 to enable the spread of polymer solution and the subsequent occurrence of discontinuous dewetting. The PVA solution was deposited on the hydrophobic substrate patterned with hydrophilic outlines, and then the patterned ultrathin PVA films were obtained through the pinning of the three-phase contact line of polymer solution as shown in Figure S2. Figure S2 shows that the gray level gradually decreases with the decreasing size of the pattern for three types of patterned substrates, indicating that the thickness of the PVA film decreases with the decreasing size of the pattern.<sup>22</sup>

The morphology and thickness of ultrathin PVA film are characterized by the AFM tapping mode. Figure 2 shows three-dimensional AFM images of the ultrathin PVA films in the form of a circle, square, and equilateral triangle. The results of Figure

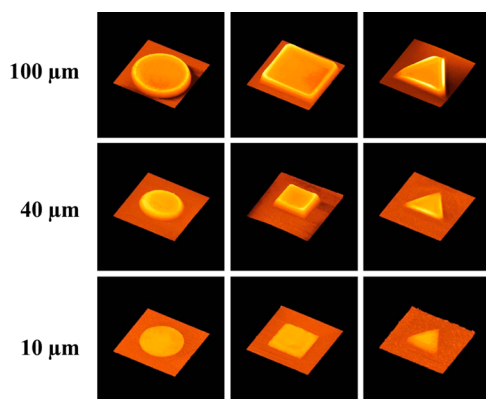


**Figure 2.** Three-dimensional AFM images (from top to bottom:  $115 \times 115$ ,  $70 \times 70$ , and  $20 \times 20 \mu\text{m}^2$ ) of ultrathin PVA films in the form of a circle, square, and equilateral triangle, obtained from PVA solution (35 mg/mL). The sizes of the patterns (from top to bottom) are 100, 40, and 10  $\mu\text{m}$ .

2 indicate that the film thickness decreases with the decreasing size of the pattern for all of three types of patterned substrates, displaying consistency with the tendency as shown in Figure S2. A noteworthy feature in Figure 2 shows that patterned substrates with sizes of 100 and 40  $\mu\text{m}$  lead to the formation of concave-shaped ultrathin PVA films, while a uniform ultrathin PVA film is formed on the hydrophobic substrate patterned with 10  $\mu\text{m}$  hydrophilic outlines.

We have also studied the thicknesses of the ultrathin PVA films formed on the substrates patterned with hydrophilic outlines of the same size, which have varying center-to-center distances ( $2R$ ,  $2.5R$ , and  $3R$ ). We observe that the thicknesses of PVA films are indistinguishable, and thus the effect of the center-to-center distance can be neglected. Figure 3a shows the

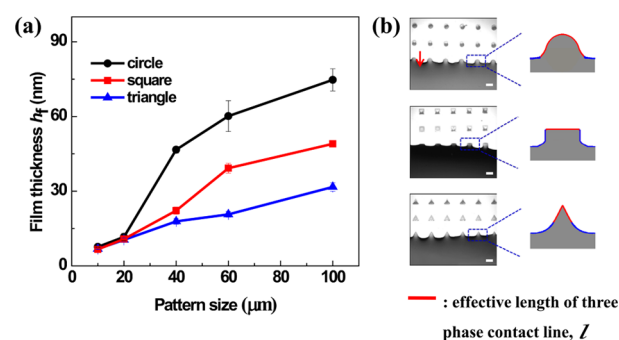


**Figure 3.** (a) Thickness of the patterned ultrathin PVA film, obtained from PVA solution (35 mg/mL), as a function of the size of the pattern. (b) The left panel shows optical micrographs of the discontinuous dewetting of PVA solution on the hydrophobic substrates patterned with hydrophilic outlines of circle, square, and equilateral triangle (from top to bottom). The red arrow indicates the direction of discontinuous dewetting. The scale bar is 50  $\mu\text{m}$ . Schematic illustrations of close-up views of hydrophilic outlines highlighted by the blue rectangles are shown in the right panel.

resulting thickness of the ultrathin PVA film as a function of the size of the pattern for three types of patterned substrates. Two features are noteworthy. First, the film thickness gradually decreases with the decreasing size of the pattern for all of the patterned substrates. Second, for three types of patterned substrates with the same pattern size (larger than 20  $\mu\text{m}$ ), the film thickness gradually decreases from the circle- to the square- and equilateral triangle-shaped patterned substrates. To decipher the physical basis for the differences in the thicknesses of formed PVA films, we capture in situ the process of discontinuous dewetting of PVA solution on three types of patterned substrates, and the results are presented in the left panel of Figure 3b. The quantity of polymer solution that can be pinned is determined by the effective length of the three-phase contact line,  $l$ , which is defined as size of the portion of the pattern interacting with the receding contact line.<sup>17</sup> The film thickness is directly proportional to the quantity of polymer solution, so the film thickness is proportional to  $l$ . Therefore, the film thickness gradually decreases with the decreasing size of the pattern for all of the patterned substrates. The right panel in Figure 4b shows a schematic illustration of the effective length of three-phase contact line (red line) of the individual hydrophilic outline, indicating the values of the effective length of three-phase contact line  $l$  (related to the size and shape of the receding contact line of the polymer solution)<sup>17</sup> for three types of patterned substrates with the same size of the pattern subject to the following tendency:  $l_c >$



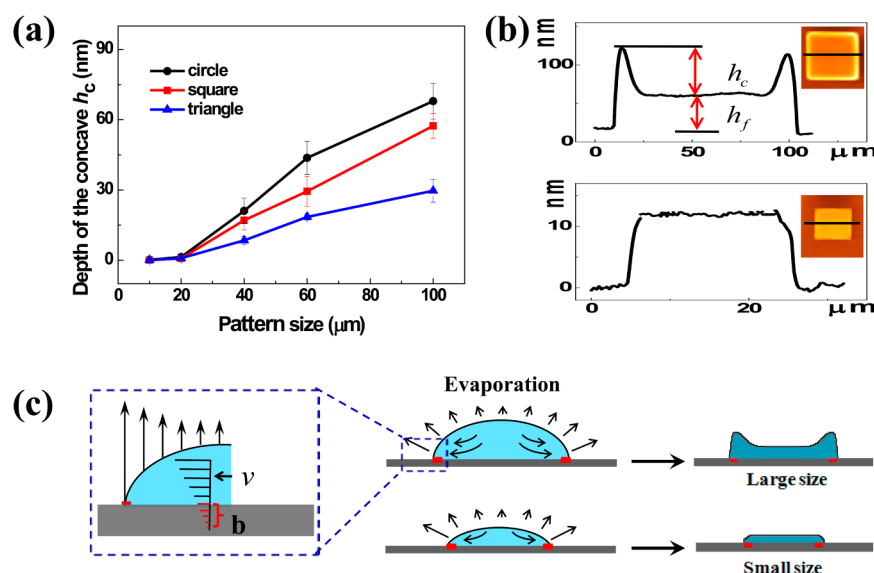


**Figure 4.** (a) Depths of the concave-shaped ultrathin PVA films formed on three types of substrates with different pattern sizes. (b) Line profiles of the concave-shaped and uniform ultrathin PVA films, in which  $h_c$  denotes the depth of the concavity and  $h_f$  denotes the film thickness, and the corresponding AFM images are shown in the insets. (c) Schematic illustration showing the lateral view of the patterned film of polymer solution formed on the hydrophobic substrate (gray) patterned with a hydrophilic outline (red). The scheme highlighted by the blue dashed line exhibits the detailed evaporation process near the contact line, in which  $b$  is the slip length defined as the distance between the solid–liquid interface and the point where the velocity gradient,  $v$ , extrapolates to zero. After the evaporation process, concave-shaped, uniform ultrathin polymer films are formed on the hydrophobic substrates patterned with large and small hydrophilic outlines, respectively.

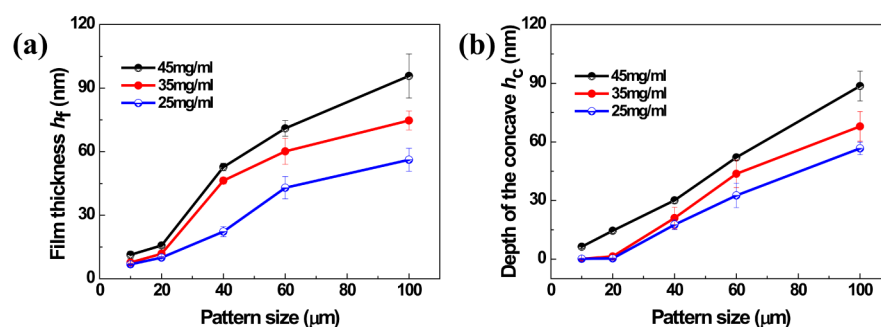


**Figure 5.** Thickness (a) and depth (b) of the patterned PVA film induced by varying concentrations of PVA solution as a function of the size of the circle-shaped pattern.

$l_s > l_v$  where  $l_c$ ,  $l_s$ , and  $l_t$  denote the effective length of three-phase contact line of circle, square, and equilateral triangle patterns, respectively. Thus, the thickness of the PVA film induced by the same size of the pattern shows the corresponding tendency:  $h_f$  (circle)  $>$   $h_f$  (square)  $>$   $h_f$  (triangle), where  $h_f$  denotes the thickness of the formed PVA film (Figure 3a). The differences in the thicknesses of three types of patterned ultrathin PVA films are still present even though the size of the pattern is smaller than  $20 \mu\text{m}$ . When the size of the pattern is  $10 \mu\text{m}$ , the thicknesses of the PVA films are  $7.7 \pm 0.27$ ,  $6.8 \pm 0.18$ , and  $6.7 \pm 0.38 \text{ nm}$  for the patterned substrates of circle, square, and equilateral triangle, respectively.

Figure 4 shows that the size of the hydrophilic outline markedly affects the morphology of the polymer film. The hydrophobic substrates patterned with hydrophilic outlines of large sizes lead to the formation of concave-shaped polymer films ( $h_c > 0$ ) (Figure 4a and the top inset in Figure 4b) because of the following contributing factors. First, solvent evaporation results in the migration of polymer chains toward the three-phase contact line due to the coffee ring effect, which is ascribed to the capillary flow in which the pinning of the

contact line of the drying drop guarantees that liquid evaporating from the edge is replenished by the liquid flowing from the interior.<sup>23–25</sup> Second, during the evaporation process, the mobility of a polymer chain in the hydrophobic domain is greater than that on the hydrophilic outlines, which enhances the outward flow of polymer solution from the interior and the associated migration of polymer chains toward the hydrophilic outline<sup>5–7</sup> (Figure 4c), further intensifying the coffee ring effect.

The results in Figure 4a show that the depth of the concave-shaped PVA film,  $h_c$ , decreases with the decreasing size of the pattern for each of three types of substrates. When the size of the pattern is less than a certain value ( $\leq 20 \mu\text{m}$ ), uniform ultrathin polymer films ( $h_c \approx 0$ ) are formed on the hydrophobic substrates (Figure 4a and the bottom panel in Figure 4b). And this is rationalized by considering the competition between the diffusion flux of polymer and the convective flux induced by the coffee ring effect. As discussed above, the thickness of the polymer solution decreases with the decreasing size of the hydrophilic outline. The shortened evaporation process and the associated convective flux caused

by the decreasing thickness of the polymer solution lead to the decrease in depth of the concave-shaped PVA films. When the thickness reduces to such an extent that the diffusion flux of polymer becomes much larger than the convective flux induced by the coffee ring effect, the solute concentration in the droplet is uniform and thus there will be no coffee ring effect.

In order to investigate the effect of varying the concentration of PVA solution on the thickness and depth of the formed PVA film, different concentrations of PVA solution are used to prepare the patterned ultrathin PVA films. However, discontinuous dewetting cannot occur when the concentration/viscosity of polymer solution is too high, such as 55 mg/mL. On the other hand, when the concentration/viscosity of polymer solution is too low, the continuous ultrathin polymer films cannot be formed and the polymer deposits only on the hydrophilic outline. Thus, a lower concentration (e.g., 10 mg/mL or less) cannot be used to prepare thinner polymer films. The viscosities of varying concentrations of the PVA solution are shown in Table S1. Thus, three different concentrations of 25, 35, and 45 mg/mL are used to prepare the patterned ultrathin PVA films, and the results are presented in Figure 5. From Figure 5a, the thickness of the formed PVA film increases with the increasing concentration of PVA solution. This could be ascribed to the increasing trapped solution, which is induced by the increasing viscosity of solution, and the decreasing velocity of the discontinuous dewetting resulted from the increasing concentration of PVA solution.<sup>26,27</sup> The prolonged evaporation process caused by the increasing trapped solution intensified the coffee ring effect, resulting in the increase of depth of the concave-shaped PVA film (Figure 5b). The depths of the concave-shaped PVA films approach zero for 20 and 10  $\mu\text{m}$  circle patterns when the concentrations of PVA solution are 25 and 35 mg/mL, indicating that the ultrathin PVA films are uniform. When increasing the concentration of PVA solution to 45 mg/mL, the depths of the concave-shaped PVA films are larger than zero, whereas we can infer that the uniform ultrathin PVA film will be formed when the size of the pattern is smaller than a critical threshold. This critical value can be derived as follows. The evaporation speed of a droplet is given by  $J = D_g/L$ , where  $D_g$  is the diffusion constant in air and  $L$  is the size of the sample due to the interference of vapor coming from many droplets on the patterned substrate (in our experiment  $L = 1$  cm). The drying time is expressed by  $\tau_{\text{dry}} = h/J = Lh/D_g$ , where  $h$  denotes the initial thickness of a droplet.<sup>28–30</sup> The diffusion time of polymer in the radial direction is given by  $\tau_{\text{diff}} = R^2/D_l$ , where  $R$  is the radius of the base circle and  $D_l$  is the diffusion constant in the liquid.<sup>31,32</sup> The influences of slip length and coffee ring effect are negligible, and uniformly patterned ultrathin polymer films can be formed for all polymer concentrations if  $\tau_{\text{diff}} < \tau_{\text{dry}}$ , i.e.,  $R^2 < (D_l/D_g)Lh$ . If  $h = 4$   $\mu\text{m}$ ,  $L = 1$  cm, and  $D_l/D_g = 10^{-4}$ , then the above condition yields  $R < 2$   $\mu\text{m}$ .

Although PVA is selected as a model polymer in this study, another water-soluble polymer such as poly(acrylic acid) (PAA) is also employed to fabricate the patterned ultrathin polymer film, showing similar properties of the film to PVA, with the thickness and depth of the patterned PAA ultrathin film decreasing with a decreasing pattern size (Figure S3).

## CONCLUSIONS

Patterned ultrathin polymer films were fabricated on hydrophobic substrates with patterned hydrophilic outlines. The thickness of the ultrathin polymer film and the depth of the

concave-shaped film can be adjusted by controlling the size of the hydrophilic outline and the concentration of the PVA solution. Decreasing sizes of patterned hydrophilic outlines and the concentration of polymer solution lead to a much thinner film and a shallower depth of the concave-shaped film. When the film thickness decreases to a certain threshold, the influences of the slip length and the coffee ring effect on the depth of the concave films can be neglected, resulting in the formation of a uniform ultrathin polymer film. The patterned ultrathin polymer film with controlled morphology and thickness would have promising applications in diverse fields such as polymer thin-film transistors and sensors.

## ASSOCIATED CONTENT

### Supporting Information

Optical images of three types of patterned substrates before stripping the photoresist and the corresponding patterned ultrathin PVA films formed on the patterned substrates. Optical images of the patterned ultrathin PAA films formed on the patterned substrates and the corresponding AFM height and 3D images of the circle-shaped ultrathin PAA films. This material is available free of charge via the Internet at <http://pubs.acs.org>.

## AUTHOR INFORMATION

### Corresponding Author

\*E-mail: [wangj220@iccas.ac.cn](mailto:wangj220@iccas.ac.cn).

### Notes

The authors declare no competing financial interest.

## ACKNOWLEDGMENTS

We acknowledge financial support from the Chinese National Nature Science Foundation (grant nos. 51173196 and 21373234) and the 973 Program (nos. 2012CB933801 and 2013CB933004).

## REFERENCES

- (1) Li, L. Q.; Gao, P.; Baumgarten, M.; Müllen, K.; Lu, N.; Fuchs, H.; Chi, L. F. High Performance Field-Effect Ammonia Sensors Based on a Structured Ultrathin Organic Semiconductor Film. *Adv. Mater.* **2013**, *25*, 3419–3425.
- (2) Horii, Y.; Ikawa, M.; Sakaguchi, K.; Chikamatsu, M.; Yoshida, Y.; Azumi, R.; Mogi, H.; Kitagawa, M.; Konishi, H.; Yase, K. Investigation of Self-Assembled Monolayer Treatment on SiO<sub>2</sub> Gate Insulator of Poly(3-hexylthiophene) Thin-Film Transistors. *Thin Solid Films* **2009**, *518*, 642–646.
- (3) Fujisaki, Y.; Ito, H.; Nakajima, Y.; Nakata, M.; Tsuji, H.; Yamamoto, T.; Furue, H.; Kurita, T.; Shimidzu, N. Direct Patterning of Solution-Processed Organic Thin-Film Transistor by Selective Control of Solution Wettability of Polymer Gate Dielectric. *Appl. Phys. Lett.* **2013**, *102*, 153305.
- (4) Li, L.; Gao, P.; Wang, W.; Müllen, K.; Fuchs, H.; Chi, L. Growth of Ultrathin Organic Semiconductor Microstripes with Thickness Control in the Monolayer Precision. *Angew. Chem., Int. Ed.* **2013**, *52*, 12530–12535.
- (5) Meredig, B.; Salleo, A.; Gee, R. Ordering of Poly(3-hexylthiophene) Nanocrystallites on the Basis of Substrate Surface Energy. *ACS Nano* **2009**, *3*, 2881–2886.
- (6) Destri, G. L.; Keller, T. F.; Catellani, M.; Punzo, F.; Jandt, K. D.; Marletta, G. Crystalline Monolayer Ordering at Substrate/Polymer Interfaces in Poly(3-hexylthiophene) Ultrathin Films. *Macromol. Chem. Phys.* **2011**, *212*, 905–914.
- (7) Ma, Y.; Hu, W.; Reiter, G. Lamellar Crystal Orientations Biased by Crystallization Kinetics in Polymer Thin Films. *Macromolecules* **2006**, *39*, 5159–5164.

- (8) Ikawa, M.; Yamada, T.; Matsui, H.; Minemawari, H.; Tsutsumi, J.; Horii, Y.; Chikamatsu, M.; Azumi, R.; Kumai, R.; Hasegawa, T. Simple Push Coating of Polymer Thin-Film Transistors. *Nat. Commun.* **2012**, *3*, 1176.
- (9) Rietveld, I. B.; Kobayashi, K.; Yamada, H.; Matsushige, K. Process Parameters for Fast Production of Ultra-Thin Polymer Film with Electrospray Deposition under Ambient Conditions. *J. Colloid Interface Sci.* **2009**, *339*, 481–488.
- (10) Xue, L. J.; Han, Y. C. Pattern Formation by Dewetting of Polymer Thin Film. *Prog. Polym. Sci.* **2011**, *36*, 269–293.
- (11) Janes, D. W.; Katzenstein, J. M.; Shanmuganathan, K.; Ellison, C. J. Directing Convection to Pattern Thin Polymer Films. *J. Polym. Sci., Part B: Polym. Phys.* **2013**, *51*, 535–545.
- (12) Zhang, Z. X.; Wang, Z.; Xing, R. B.; Han, Y. C. Patterning Thin Polymer Films by Surface-Directed Dewetting and Pattern Transfer. *Polymer* **2003**, *44*, 3737–3743.
- (13) Zhang, Z. X.; Wang, Z.; Xing, R. B.; Han, Y. C. How to Form Regular Polymer Microstructures by Surface-Pattern-Directed Dewetting. *Surf. Sci.* **2003**, *539*, 129–136.
- (14) Hong, S. W.; Byun, M.; Lin, Z. Q. Robust Self-Assembly of Highly Ordered Complex Structures by Controlled Evaporation of Confined Microfluids. *Angew. Chem., Int. Ed.* **2009**, *48*, 512–516.
- (15) Chou, S. Y.; Zhuang, L.; Guo, L. J. Lithographically Induced Self-Construction of Polymer Microstructures for Resistless Patterning. *Appl. Phys. Lett.* **1999**, *75*, 1004–1006.
- (16) Jackman, R. J.; Duffy, D. C.; Ostuni, E.; Willmore, N. D.; Whitesides, G. M. Fabricating Large Arrays of Microwells with Arbitrary Dimensions and Filling Them Using Discontinuous Dewetting. *Anal. Chem.* **1998**, *70*, 2280–2287.
- (17) Cheng, D. F.; McCarthy, T. J. Using the Fact that Wetting Is Contact Line Dependent. *Langmuir* **2011**, *27*, 3693–3697.
- (18) Arnold, F. E.; Deusen, R. L. V. Unusual Film-Forming Properties of Aromatic Heterocyclic Ladder Polymers. *J. Appl. Polym. Sci.* **1971**, *15*, 2035–2047.
- (19) Ortiz-Young, D.; Chiu, H.-C.; Kim, S.; Voitchovsky, K.; Riedo, E. The Interplay between Apparent Viscosity and Wettability in Nanoconfined Water. *Nat. Commun.* **2013**, *4*, 2482.
- (20) Tsai, P.; Peters, A. M.; Pirat, C.; Wessling, M.; Lammertink, R. G. H.; Lohse, D. Quantifying Effective Slip Length over Micro-patterned Hydrophobic Surfaces. *Phys. Fluids* **2009**, *21*, 112002.
- (21) Maali, A.; Bhushan, B. Measurement of Slip Length on Superhydrophobic Surfaces. *Philos. Trans. R. Soc. A* **2012**, *370*, 2304–2320.
- (22) Poelma, J. E.; Fors, B. P.; Meyers, G. F.; Kramer, J. W.; Hawker, C. J. Fabrication of Complex Three-Dimensional Polymer Brush Nanostructures through Light-Mediated Living Radical Polymerization. *Angew. Chem., Int. Ed.* **2013**, *52*, 6844–6848.
- (23) Deegan, R. D.; Bakajin, O.; Dupont, T. F.; Huber, G.; Nagel, S. R.; Witten, T. A. Capillary Flow as the Cause of Ring Stains from Dried Liquid Drops. *Nature* **1997**, *389*, 827–829.
- (24) Deegan, R. D.; Bakajin, O.; Dupont, T. F.; Huber, G.; Nagel, S. R.; Witten, T. A. Contact Line Deposits in an Evaporating Drop. *Phys. Rev. E* **2000**, *62*, 757–765.
- (25) Shen, X. Y.; Ho, C. M.; Wong, T. S. Minimal Size of Coffee Ring Structure. *J. Phys. Chem. B* **2010**, *114*, 5269–5274.
- (26) Redon, C.; Brochard-Wyart, F.; Rondelez, F. Dynamics of Dewetting. *Phys. Rev. Lett.* **1991**, *66*, 715–718.
- (27) Shull, K. R.; Karis, T. E. Dewetting Dynamics for Large Equilibrium Contact Angles. *Langmuir* **1994**, *10*, 334–339.
- (28) Kobayashi, M.; Makino, M.; Okuzono, T.; Doi, M. Interference Effects in the Drying of Polymer Droplets on Substrate. *J. Phys. Soc. Jpn.* **2010**, *79*, 044802.
- (29) Ozawa, K.; Okuzono, T.; Doi, M. Diffusion process during drying to cause the skin formation in polymer solutions. *Jpn. J. Appl. Phys.* **2006**, *11*, 8817–8822.
- (30) Kobayashi, M.; Okuzono, T.; Doi, M. Final shape of a drying thin film. *Phys. Rev. E* **2009**, *80*, 021603.
- (31) Okuzono, T.; Aoki, N.; Kajiya, T.; Doi, M. Effects of Gelation on the Evaporation Rate of Polymer Solutions. *J. Phys. Soc. Jpn.* **2010**, *79*, 094801.
- (32) Jung, Y.; Kajiya, T.; Yamaue, T.; Doi, M. Film Formation Kinetics in the Drying Process of Polymer Solution Enclosed by Bank. *Jpn. J. Appl. Phys.* **2009**, *48*, 031502.